

Technical Articles

- Fast Breeder Test Reactor: Attainment of Design Power of 40 MWt

Young Officer's Forum

- Deformation-Induced Ferrite Transformation in P92 Steel During Deformation at Elevated Temperatures

Young Researcher's FORUM

- Nitrogen as an Electron Accepting Host in Pnicogen Bonding: A Comprehensive Study using Matrix Isolation Infrared Spectroscopy and Quantum Chemical Computations

News and Events

- National Hindi Scientific Seminar (NHSS-2022)
- International Conference on Recent Advances in High Pressure Science and Technology (ICReACh-2022)
- Theme Meeting on Computational Modelling of Nuclear Reactor Materials
- 5th National Conference URJAVARAN – 2022

Awards, Honours and Recognitions

Director's Message

Dear Readers,

It gives me immense pleasure to announce FBTR attaining the designated power of 40MWt on 07-03-2022. This event will be etched in the history of the Indian fast reactor program. I dedicate this achievement to every individual, past and present, who has contributed to the growth of the fast breeder program from IGCAR. Starting with 22 fuel sub-assembly (SA) core rated 10 MWt, the FBTR team has indigenously designed a novel core with MARK-1 fuel SAs and a few poison SAs to raise the power to 40 MWt and successfully connect to the Grid.

FBTR would continue to provide valuable inputs to the fast reactor program through irradiation of metallic fuels, structural materials, and human resource development. FBTR also serves as a source for generating radioactive isotopes Sr⁸⁹ and P³², useful for societal applications.

I welcome readers to a technical article on FBTR attaining 40 MWt and a column by a young officer and a research scholar. The back cover has a Paddyfield Pipit with its prey photographed near MS Swaminathan Research Plant in DAE Complex, Kalpakkam.

I appreciate the efforts of the editorial committee and the authors for their contributions to the newsletter.

(B. Venkatraman)
Director, IGCAR

Editor's Desk

Dear Reader

Greetings

It is my pleasant privilege to forward the latest issue of IGC Newsletter (Volume 132, April 2022, Issue 2). I thank my team for their timely inputs, cooperation, and support in bringing out this issue.

The digital copy is published through the websites <http://vaigai> and <http://www.igcar.gov.in>. Additionally, on the Vaigai website, the flip copy of the Newsletter is available.

In this issue, we have a message from Director, IGCAR. The issue has a technical article on the FBTR attaining the designated power 40MWt, and the work of a young officer and a research scholar.

Further, I am happy to share with you the awards and honors earned by our colleagues and about the important events during January to March 2022.

The Editorial Committee would like to thank all the contributors. We look forward to receiving constructive suggestions from readers towards improving the IGC Newsletter content.

We express our deepest gratitude to Director IGCAR for his keen interest and guidance.

With best wishes and regards

S.Rajeswari

Chairman, Editorial Committee, IGC Newsletter and
Head, Scientific Information Resource Division, IGCAR

EDITORIAL COMMITTEE

Ms. S. Rajeswari,
Dr. V. S. Srinivasan,
Dr. John Philip,
Dr. T. R. Ravindran,
Dr. C. V. S. Brahmananda Rao,
Shri A. Suriyanarayanan,
Shri M. S. Bhagat,
Shri G. Venkat Kishore,
Dr. Girija Suresh,
Shri M. Rajendra Kumar,
Shri S. Kishore, Shri Biswanath Sen,
Dr. N. Desigan,
Shri Gaddam Pentaiah
Shri K. Varathan

ISSN 0972-5741

Volume 132, Issue 2, April 2022:

Published by Scientific Information Resource Division, SQ&RMG, IGCAR, Kalpakkam-603102

Fast Breeder Test Reactor: Attainment of Design Power of 40 MWt

Fast Breeder Test Reactor (FBTR) is a loop type, sodium cooled, experimental fast reactor with design power of 40 MWt (13.2 MWe) and has been in operation since 1985 at various power levels up to 32 MWt till 29th irradiation campaign.

The core of FBTR was originally designed with 65 fuel sub-assemblies (FSAs) of MOX with 30% PuO₂+ 70% UO₂ with latter enriched to 85% U-235. Due to various reasons, enriched uranium could not be procured from France as originally envisaged. As an alternative fuel, high Pu + Natural U mixed carbide fuel was chosen because of its excellent compatibility with sodium, high thermal conductivity, good irradiation behaviour and breeding potential. FBTR was made critical with a small core rated for 10.5 MWt consisting of 22 Mark-I (70% PuC + 30% UC) FSAs in October 1985. The reactor power was progressively increased by adding more FSAs and increasing the operating Linear Heat Rate (LHR) based on encouraging results of Post Irradiation Examination (PIE) of FSAs discharged at burn-ups of 25, 50 and 100 GWd/t and out-of-pile studies. The maximum power of 32 MWt could be achieved in the 27th campaign in September 2018. During this period, all variants of carbide fuel viz. Mark I (HG), Mark I (PHWR), Mark II (55% PuC + 45% UC) and MOX fuel (44% PuO₂ + 56% Natural UO₂) have been introduced into the core and valuable irradiation data obtained.

Transition From 29th Campaign to 30th Campaign

With MK I Carbide FSA alone, FBTR core could not be expanded beyond 56 FSAs due to minimum shutdown margin (SDM) criterion and hence a novel concept was proposed to introduce four Boron Carbide poison SAs in the second ring to increase the core size beyond 56 FSA. The power produced from this core was estimated to be more than 40 MWt. This concept was approved by AERB and subsequently Safety Report was prepared for this core and submitted. After detailed review, the safety analysis report was accepted by Regulators.

After obtaining the SARCPA approval, transition to 30th irradiation campaign core was planned in six fuel handling steps. After each fuel handling step, physics parameters like SDM, control rod

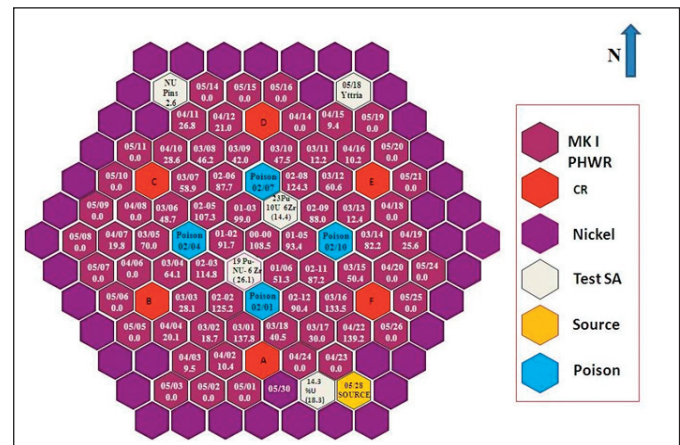


Figure 1: Core configuration with 68 MK-I FSA

(CR) worth and critical heights were measured. The total power from this 68 FSA core was estimated to be 42.6 MWt with peak rated FSA at 03-02 location operating at LHR of 400 W/cm. The estimated SDM and CR worth were 4693 pcm and 9484 pcm respectively.

Fuel Handling Campaigns (FHC) for transition of core for the commencement of the 30th campaign was commenced in October 2021 and completed in February 2022. The details of FSAs charged/discharged are presented in Table 1. One FSA transferred to periphery in step 1 is brought back to core in step 3. In all 27 MK I FSAs and 4 poison SAs were loaded into the reactor core. 8 MOX SAs and 3 MK I FSAs which reached target burn-up were transferred to storage locations for cooling.

Table 1 Fuel handling details

	FH Step					
	1	2	3	4	5	6
No. of FSA discharged	8	0	1	1	2	0
No. of fresh FSA charged	8	0	3	6	6	4
No. of poison SA loaded	0	1	0	1	2	0

Out of 68 FSAs, 27 are fresh MK I and among these 27 fresh FSAs, 8 were loaded in the 4th ring and 19 were loaded in the 5th



Figure 2 SG tubes in blanked condition



Figure 3 SG tubes in normalized condition



Figure 4 Revamped Main Cooling Tower

ring. Between step 2 and step 5, 4 poison SAs were loaded in second ring at 02-01, 02-04, 02-07 and 02-10 locations.

Startup and Physics Experiments

After each FHC, reactor was made critical and criticality was followed by control rod calibration to derive the SDM. After final FHC (Step 6), the reactor was made critical on 22nd February and control rod calibration done. The measured value of CR worth was 6685 pcm and derived value of SDM from the measured CR worth was 4485 pcm which is above the Technical Specification limit. The measurement of Isothermal temperature coefficient was carried out and the value is -3.47 ± 0.17 pcm/ $^{\circ}$ C. Raising of reactor power was started along with power coefficient measurement till maximum design power of 40 MWt was reached on 7th March, 2022 at 17:30 h. The measured value of power coefficient is -7.06 pcm/MWt. The measured value of temperature and power coefficients are well above the estimated values adhering to Technical Specification limits.

Upgradations and Modifications of Systems

Normalization of tubes in steam generator modules

In order to operate the reactor near design temperature at lower reactor power levels, 3 out of 7 tubes in each SG module were blanked in 2008. For raising the reactor power to 40 MWt, these tubes were normalized. After normalization, qualification of weld joints was done as per procedure.

Additional LOR parameter on “Reactor vessel sodium inlet temperature high”

In case of loss of feed water flow to any one SG loop, reactor inlet sodium temperature will increase and introduce negative feedback effect in the core. The reduced core heat will be removed by the other SG loop which will be operating with increased feed water flow and reactor will continue to operate. However, because of the mismatch between core heat and heat removal, primary sodium inlet temperature will increase. This will also introduce a hot shock of ~ 0.6 $^{\circ}$ C/s in the other loop Intermediate Heat Exchanger (IHX) and a large temperature difference ~ 134 $^{\circ}$ C between primary sodium flow stream at the common junction point (i.e., Culotte junction). In order to avoid operation of reactor in this configuration, one additional LOR parameter based on



Figure 5 Viewing window of SG casing

“High Reactor Inlet Sodium Temperature” was introduced and commissioned.

Fabrication of Poison SAs

40 MWt core configuration has four poison SAs in the second ring. Boron carbide pellets with 50% enrichment in B-10 were supplied by Heavy Water Plant, Manuguru. NFC, Hyderabad fabricated poison sub-assemblies. The design of poison SAs is such that its foot is similar to a normal SA and its head design is similar to control rod outer sheath. Each poison SA has eight B_4C pellets of size: 38 mm dia x 47 mm height and density 2.4 g/cc.

Upgradation in power supply

Before commencing the 40 MWt operation, overhauling and servicing of FBTR 10 MVA transformer was taken up and after servicing, the transformer was installed and commissioned. The 24 V DC chargers of control power supply were replaced with new chargers with advanced operating features and seismic qualification. Commissioning and testing of these chargers were completed.

Revamping of 50 MWt Main Cooling Tower

Cooling tower was completely dismantled and refurbished. The existing cooling tower splash box and cover assembly on water distribution system, PVC ‘V’ type splash bars, splash bars support grid system, PVC drift eliminators and GI corrugated louver sheets were replaced with fresh materials. After revamping, cooling tower was commissioned and put into service. Structural stability of all the internal materials was checked to be satisfactory.

High temperature viewing windows for SG casing

SG casing contains four numbers of steam generators which generate steam required for the turbo-generator. In case of actuation of sodium leak detectors in SG module, the trap doors and manholes need to be opened for inspection during operation of reactor. To avoid this, three high temperature quartz glass (rated for 1000 $^{\circ}$ C) viewing windows were installed on SG casing at suitable locations.

*Reported by
Colleagues from
Reactor Facilities Group*

Young Officer's Forum



Mantosh Mandal completed his B.Tech. in Metallurgical and Materials Engineering from NIFFT Ranchi in 2018. He joined DAE as TSO of 63rd batch OCES, BARC Training School, Mumbai. He joined the Metal Forming and Tribology Section (MFTS), MMG in 2020 as SO/C. He completed his M. Tech. in Metallurgy from Homi Bhabha National Institute in 2021. His basic research interests are hot deformation behaviour and microstructure evolution.

Deformation-Induced Ferrite Transformation in P92 Steel During Deformation at Elevated Temperatures

Various types of phases appear in metallic materials depending on the chemical composition and temperature. Each phase has distinct properties. Hence, the shape, size and location of the phase affect the overall properties of material containing the phase. One phase can transform into another phase by variation in temperature and the transformation is sometimes influenced by stress or strain. Besides these, certain phase transformations can also be induced by a combination of deformation and temperature. These transformations are relevant to steels, since they can occur during the manufacturing process.

Further, the stabilization of softer phases like ferrite in a hard and brittle phase like martensite may alter the strength and toughness of the steel during manufacturing and service. The present study reveals the occurrence of deformation-induced ferrite transformation (DIFT) in a boiler steel named 'P92' (Fe-9Cr-1.8W-0.5Mo-0.4Mn-0.06Nb-0.027V-0.12C (in wt%)) for the first time and the illustrates how DIFT can control microstructural and mechanical properties of the steel.

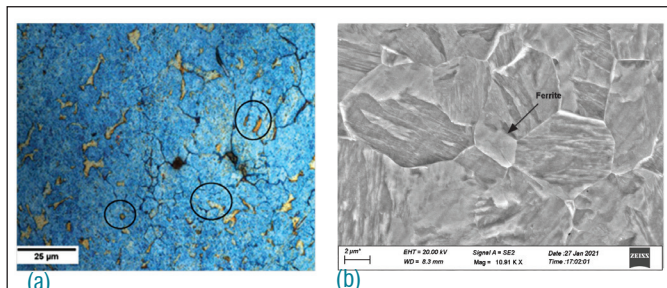


Figure 1: Formation of ferrite after soaking at 1173K for 50 min. Revealed by (a) colour tint etching(b) surface contrast in SEM.

The influence of thermomechanical processing on initiation and propagation of DIFT are investigated.

Ferrite after isothermal heat treatment

Some ferrite is observed during isothermal heat treatment near A_3 temperature, as shown in Figure 1. These ferrite are either diffusional ferrite or retained ferrite. For phase identification, colour tint etching is carried out using Beraha's sulfamic acid reagent no. 4. The martensite phase is coloured blue while ferrite is white.

The fraction of ferrite formed in this case is very less (2-4%), and is associated with the prior austenite grain boundaries.

Ferrite after thermomechanical treatment

Upon deforming the specimens to 50%, at 1173K, significant amounts of deformation-induced ferrite is observed in the microstructure (Figure 2).

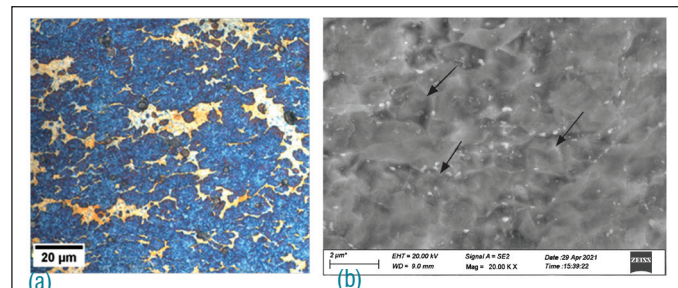


Figure 2: Formation of ferrite after deformation at 1173K with 10s⁻¹ strain rate. Revealed by (a) colour tint etching(b) surface contrast in SEM.

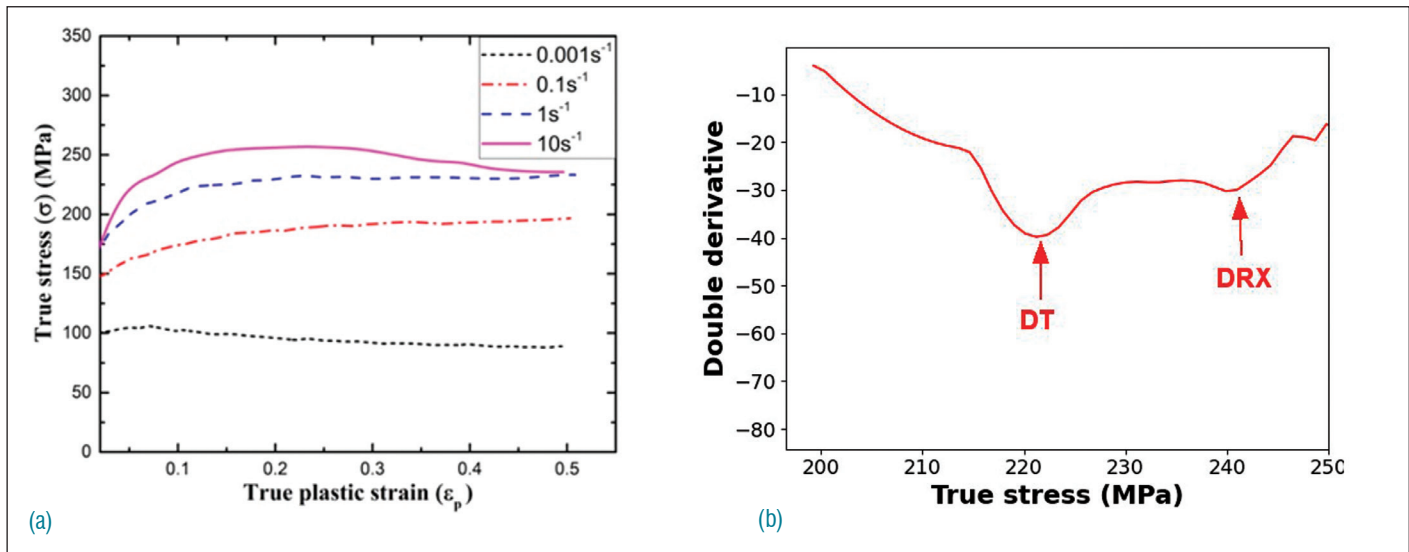


Figure 3: (a) Stress-strain curves at 1173K, (b) $\frac{\delta\theta}{\delta\sigma}$ vs σ curve at 1173K at strain rate 10s-1.

The deformation-induced ferrite forms in clusters which are not specifically associated with prior austenite boundaries. At high magnification, one such cluster shows the presence of several ultrafine ($\leq 1 \mu\text{m}$) polygonal cells.

The microstructure of steel affects the stress-strain behaviour of the steel. Some researchers reported that if there is strain-induced ferrite transformation, the work hardening rate decreases linearly with the true stress, with an inflection point due to softening mechanism. In case of DIFT/DT there would be two minima in $\delta\theta/\delta\sigma$ with σ plot. The first minima can be correlated to dynamic transformation and the second minima can denote dynamic recrystallization. The critical stress can be calculated at the minima by the following equation:

$$\delta/\delta\sigma (\delta\theta/\delta\sigma)=0$$

Figure 3(a) shows that flow stress increases with an increase in the strain rate during deformation at 1173K. The rise in flow stress is attributed to the dislocation multiplication induced by increased rate of deformation. For confirmation $\delta\theta/\delta\sigma$ with σ curve has been plotted as shown in Figure 3(b), it shows two minima at deformation at 10s-1. The presence of two minima in the curve shows there is formation of deformation-induced ferrite.

EBSM analysis of deformation-induced ferrite

The crystallographic features of the DIFT- α and the nature of α/α interfaces were further investigated using EBSD studies. An IPF map corresponding to the compression axis is shown in Figure 4 (a). The colours on the map represent crystallographic orientations at each point. These orientations of the martensite (α)/ferrite (α) are linked to the orientations of the parent austenite (γ) through an

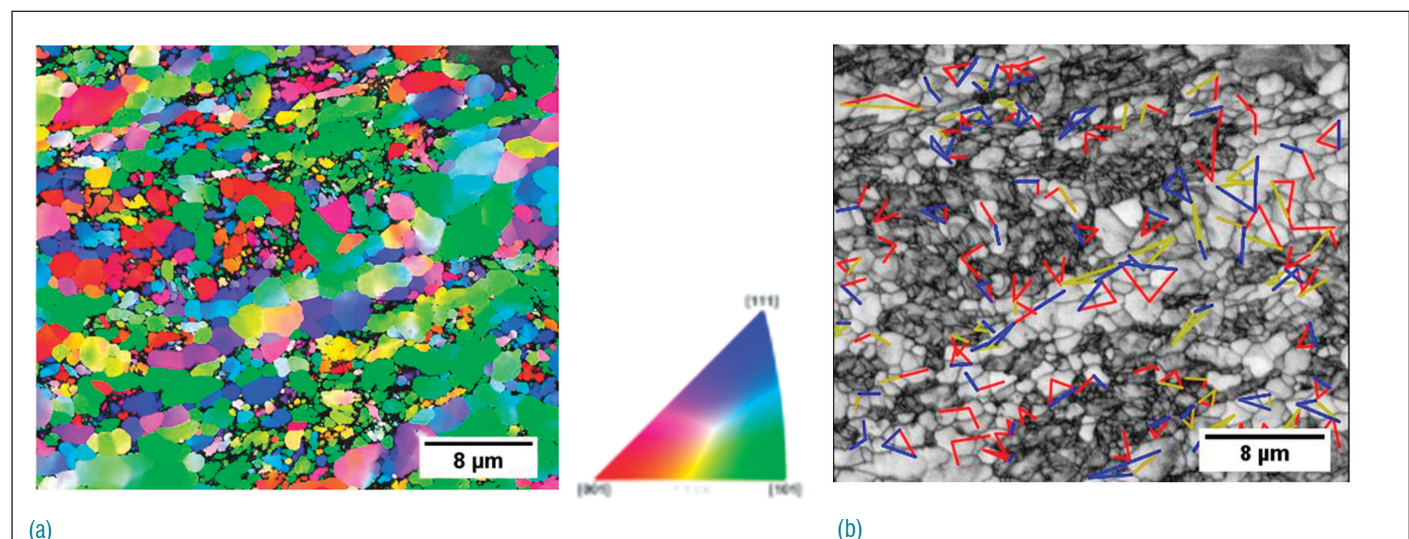


Figure 4: (a) IPF map corresponding to compression axis, (b) orientation relation marked in band contrast map.

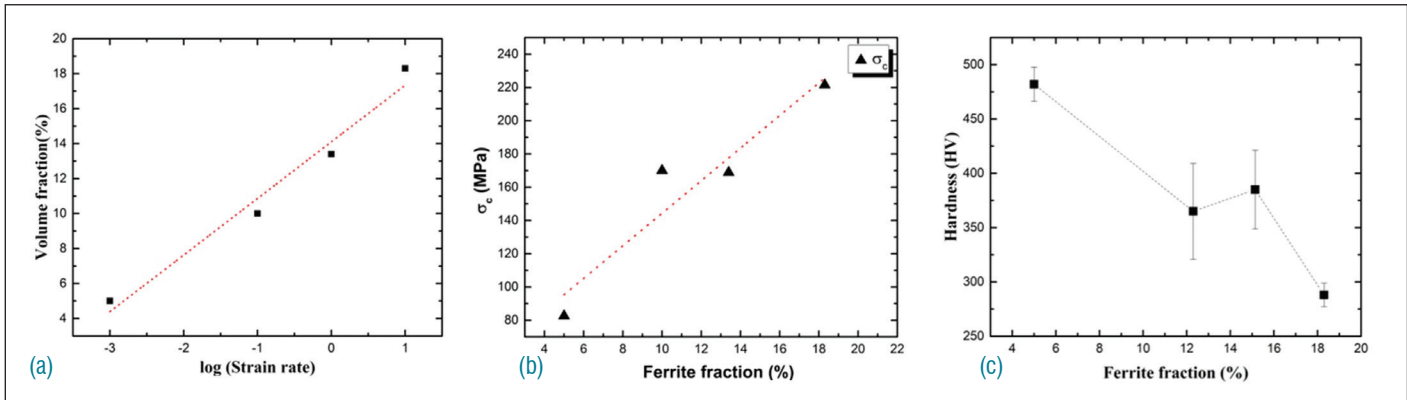


Figure 5: Change in ferrite fraction with (a) strain rate, (b) critical stress for DIFT, (c) influence of ferrite volume fraction on hardness.

orientation relationship (OR). The OR can be used to infer the origin of martensite and ferrite regions in the microstructure and thereby to explain the mechanics of the strain-induced transformation.

For neighbouring daughter crystals A, B and C, the misorientations (Δg_{AB} , Δg_{BC} , Δg_{AC}) is compared with a list of theoretical misorientations (termed 'operators') derived from the OR. If the measured misorientations consistently match a set of operators ($O = \{O_i, O_j, \dots\}$), then the daughter crystals are derived from the same parent grain. This can be used to determine if neighbouring α/α' crystals formed from the same parent γ grain, within specified angular tolerances. In order to test this, a band contrast map as shown in Figure 4(b) was used. In the band contrast map, martensite regions appear darker because of inherent high strain, whereas ferrite regions appear light due to lesser strain. Sets of neighbouring crystals were tested for the presence of a shared OR and the results were marked on the band contrast map.

Blue and yellow lines join crystals that are calculated to have formed from the same parent γ grain (allowed angular tolerances for blue and yellow are 10° and 15° respectively) while red lines join crystals that form from different parent γ grains (outside the 15° tolerance). Upon quantitative examination of Figure 3 (b), it is found that the α forms in two morphologies; large regions of continuous α (termed 'rafts') which are not related to the neighbouring α' by ORs and ultrafine α grains surrounded by a matrix of α' which share a common OR within 15° tolerance.

Driving force for DIFT

During deformation, defects accumulate in the austenite grains, which are the nucleation sites for ferrite formation. It has been

considered that these defects raise the Gibbs free energy and destabilize the austenite and transform it into ferrite. It is also justified by the fact that the volume fraction of ferrite increases with an increase in strain rate, as shown in Figure 5(a). With an increase in strain rate, more defects accumulate in the austenite grains, nucleating more ferrite grains.

The amount of DIFT ferrite is reported to increase with the critical stress (σ_c) at which DIFT initiates.

This is verified in Figure 5(b) across a wide range of strain rates, although the relationship is not monotonic.

The main reason for the refinement of ferrite grains is due to an increase in dislocation density in the austenite phase. These dislocations are the nucleation sites for the new ferrite phase. The higher strain generates more deformation defects, increasing the probability of generating very fine strain-induced ferrite grains.

Variation of hardness with volume fraction of ferrite is shown in Figure 5(c). The plot shows that the hardness of the steel is sensitive to the volume fraction of ferrite present in the steel. By controlling the volume fraction of ferrite, mechanical properties of the steel can be controlled.

In conclusion, ferrite islands in the martensite matrix can be produced by exploiting the phenomenon of deformation-induced ferrite transformation in P92 steel. The ferrite formed can be continuous or discontinuous and could be ultrafine grained. The careful control of strain rate and other thermomechanical process parameters can be used for microstructural engineering through high-temperature deformation in 9Cr steel.

Young Researcher's FORUM



Mr. Swaroop Chandra is working towards his doctoral degree from HBNI at the Radioanalytical Chemistry and Spectroscopic Studies Section, MC&MFCG, IGCAR. He completed his bachelors and masters in chemistry under the 5-year Integrated M.Sc programme at Amrita Vishwa Vidyapeetham, Coimbatore. He is studying the origins and workings of pnicogen bonds, a class of non-covalent interactions using matrix isolation infrared spectroscopy and the state-of-the-art quantum chemical computations. He has published four papers in peer-reviewed international journals so far towards his Ph.D Work. In addition, he has contributed to works published in eight other publications.

Nitrogen as an Electron Accepting Host in Pnicogen Bonding: A Comprehensive Study using Matrix Isolation Infrared Spectroscopy and Quantum Chemical Computations

Analogues of hydrogen bonding involving covalently bound atoms belonging to elements of p-block, playing electron acceptors have been explored during the last two decades. Weak interactions of the form D-X...A, wherein X is the principal electron acceptor and X...A is the weak non-covalent bond, have been recurrently found to prevail within macromolecular systems, inorganic and organic alike. When 'X' is hydrogen, the well-known hydrogen bonding is said to operate which has been studied quite extensively for more than a century. The significance of hydrogen bonding in biological systems, such as in the sustenance of the double helix structure of DNA strands, has been known well enough, that it now forms an indispensable topic of study at all levels. Hydrogen bonding is also thought to be central to the anomalous behaviour of water across phases, particularly, the lower density of ice relative to liquid water. This anomaly of water has been instrumental in ensuring that oceans, the cradles of life on earth, always remained hospitable

to life regardless of the seasons on the planet. Very much like hydrogen bonding, when 'X' is an atom belonging to the halogens, halogen bonding occurs. Similarly, when X belongs to the carbon, nitrogen, oxygen or noble gas groups, they are named as tetrel, pnicogen, chalcogen or aerogen bonds, respectively.

These interactions along with hydrogen bonding have been found to be consequences of localized anisotropies on the electrostatic potential (ESP) surrounding 'X'. The ESP, or more appropriately the molecular electrostatic potential, at a given point in the space surrounding a molecule, is the resultant of the positive nuclear potential and the negative potential due to the electron density at that point. In D – X...A, owing to the electronegativity of D, a specific region on the ESP of X is polarized positive. The location of this positively polarized region is dependent on the situation of 'D' and the kind of covalent bond that binds it with 'X'. When a σ -bond prevails between D and X, the anisotropy on X is generated on the opposite 'face' of X, collinear to the D-X bond. This feature on the ESP is termed a σ -hole (Figure 1). Nucleophiles (A) approaching X, to access the σ -hole, maintain a near linearity with respect to the D-X bond such that \angle D-X-A is close to 180° . This directionality forms a characteristic of the σ -hole driven tetrel, pnicogen, chalcogen, halogen, aerogen and even hydrogen bonds. When the bond between D and X is a π -bond, the anisotropy in ESP occurs on the π -electron cloud itself, as a π -hole, due to which the nucleophile 'A' approaches X, perpendicular to the molecular plane of D=X. In these cases \angle D-X-A always tends to 90° . In short, the non-covalent interactions mentioned so far are all electrostatic phenomena, primarily.

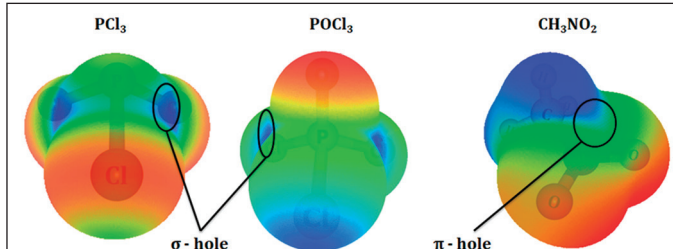


Figure 1. Projections of electrostatic potential (ESP) on 0.001 au electron density isosurface of PCl_3 (phosphorus trichloride), POCl_3 (phosphoryl chloride) and CH_3NO_2 (nitromethane). Deep blue regions are indicative of most positive ESP while deep red correspond to most negative ESP

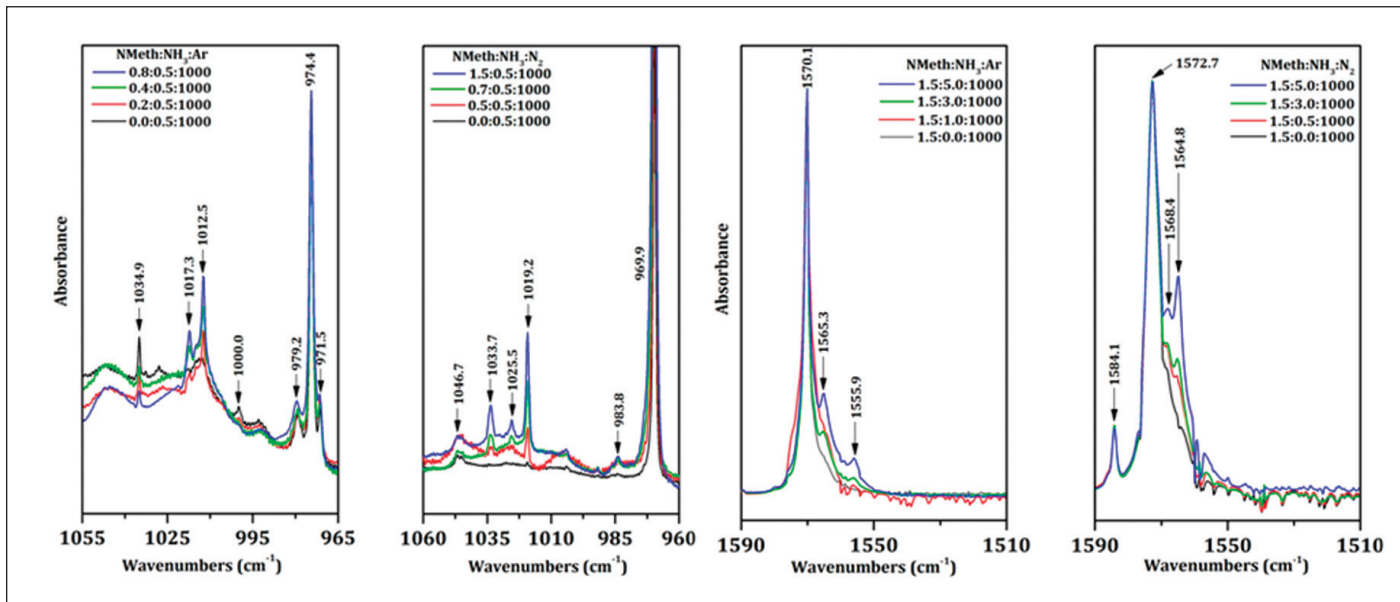


Figure 2. Infrared spectra of matrix isolated mixtures of nitromethane and ammonia at 12 K following the annealing of matrixes to 35 K. (from left), the first two grids display the N-H bending region of the IR spectra of samples isolated within Ar and N₂ matrixes respectively, while the last two display the O=N=O stretching region in Ar and N₂ respectively

Phosphorus has been of interest to research and development relevant to the nuclear industry because of the use of phosphates (tri-n-butyl phosphate, in particular) as ‘extractants’ for the reprocessing of spent nuclear fuel and the chemistry of extraction at the molecular level is quite primitively understood so far. Here, pnicogen bonding exhibited by phosphorus is a point of interest since pnicogen bonding could play a role in imparting the observed behaviour of extractants under various conditions of operation/experiment. Also, phosphorus is an element present in biological systems, predominantly in two forms: phosphates of calcium in bones and the phosphate sugar backbone of the DNA/RNA strands. Phosphorus bonding by trivalent and pentavalent phosphorus has been studied quite extensively in our group using the combination of experiments (matrix isolation infrared (IR) spectroscopy) and theory (*ab initio* and Density Functional Theory (DFT) based quantum chemical calculations), involving prototypical phosphorus trichloride (PCl₃, trivalent) and phosphoryl chloride (POCl₃, pentavalent). The presence of σ -holes around phosphorus, due to its covalent binding with chlorine in both the prototypes, has been established to be the primary cause of pnicogen bonding by phosphorus. The polarizability of phosphorus undoubtedly plays a role in the formation of σ -holes. Pnicogen bonding has been observed to gain prominence in heavier pnicogens (arsenic, antimony and bismuth), clearly due to their enhanced polarizability.

Nitrogen being the smallest of pnicogens has the lowest polarizability and thus, instances of its involvement in pnicogen bonding, as an electron acceptor, have been quite elusive, until very recently. Multiple evidences of nitrogen hosting pnicogen bonds with a variety of nucleophiles playing donors have been

obtained by investigations involving the combination of matrix isolation infrared spectroscopy and *ab initio* / DFT computations, in our laboratory. Nitromethane (CH₃NO₂), a popular solvent is the chosen prototype containing electron accepting nitrogen. The non-bonded electron pair of nitrogen is delocalized across the O=N=O moiety for the sustenance of π -bonds with the twin oxygen atoms. This deprivation of electron density by the oxygen atoms, imparts a positive electrostatic potential over nitrogen in nitromethane. The electrostatic potential (Figure 1) projected over an electron density isosurface (0.001 au, van der Waals surface), around nitromethane confirms the presence of twin π -holes over nitrogen on either side of the O=N=O plane. These π -holes facilitate the electron accepting behaviour of nitrogen, thus hosting O=N...X pnicogen bonds.

Heterodimers of nitromethane and phosphorus trichloride with ammonia have been isolated successfully within inert matrixes (Ar and N₂) maintained at 12 K. The role of pnicogen bonding, hosted by nitrogen of nitromethane and surprisingly that of ammonia too, in the preferential stabilization of specific geometries in both these systems has been proven computationally, which is reinforced by the generation of these geometries within the matrixes at low temperatures. A typical experiment involves the preparation of gas-phase mixture of the precursors (nitromethane and ammonia), containing a large excess of inert gas (Ar/N₂). This gas mixture is then deposited effusively onto a KBr substrate, transparent to infrared radiation, maintained at 12 K. The solid film obtained is then probed using a Fourier transform – IR spectrometer. The matrix is also subjected to ‘annealing’ at progressively increasing temperatures (25, 30 and 35 K for Ar; 25 and 32 K for N₂).

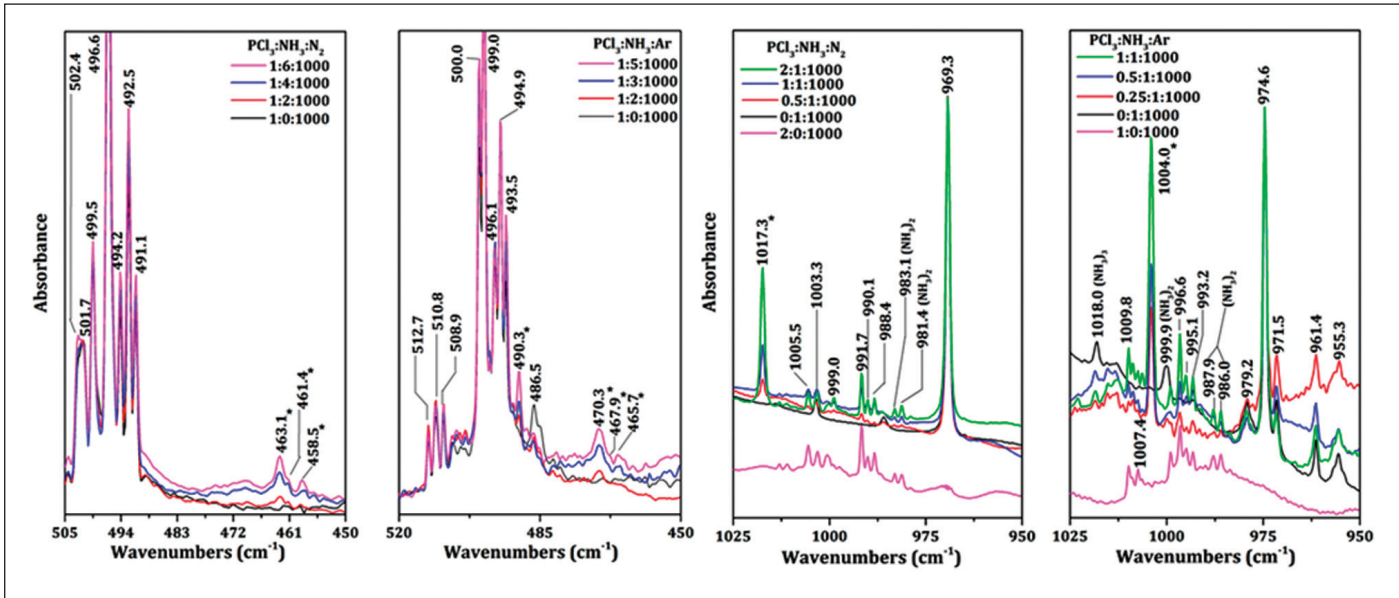


Figure 3. Infrared spectra of matrix isolated mixtures of ammonia and phosphorus trichloride at 12 K following the annealing of matrixes to 35 K. (from left), the first two grids display the P-Cl stretching region of the IR spectra of samples isolated within Ar and N₂ matrixes respectively, while the last two display the N-H bending region in Ar and N₂ respectively

The enhanced mobility of the matrix-isolated molecules during annealing allows their diffusion towards each other, resulting in the formation of heterodimers, trimers and higher clusters, depending on the relative proportion of the precursors in addition to the generation of homodimers and clusters. The proximity, of the sub-molecules within heterodimers, causes perturbations to the fundamental vibrational modes of the sub-molecules, relative to their non-interacting states. These perturbations are signatures of interactions prevailing within the heterodimer. They manifest as changes in the strength of covalent bonds within the sub-

molecules. The perturbation, of vibrational modes of a molecule, on an energetic scale, is dependent on the said strength of covalent bonds. Thus, the perturbations inflict changes in the separation of these states, in terms of energy, which are in turn observed as ‘shifts’ in the characteristic vibrational frequencies of infrared radiation absorbed (Figures 2 and 3).

The weak nature of pnicogen bonding translates to minute shifts in the absorption frequencies. The enhanced spectral resolution enabled by matrix isolation, allows the capture of these minuscule shifts by an FT-IR spectrometer. The intensity of these shifted

Table 1: Comparison of shifts, in the signature absorptions by nitromethane and ammonia submolecules in heterodimers, predicted by harmonic frequency calculations and those observed in the IR spectra of matrix isolated samples

Computed Wavenumber (cm ⁻¹)		Experimental Wavenumber (cm ⁻¹)				Mode Assignment
		Ar		N ₂		
v	Δv	v	Δv	v	Δv	
N-H Bending						
1042.8 (131)	---	974.4	---	969.9	---	v ₂ of NH ₃ monomer
1100.8 (144)	+58.0	1012.5	+38.1	1019.2	+49.3	N-H bending in NM-AM I dimer
		1017.3	+42.9	1025.5	+55.6	N-H bending in NM-AM I dimer
1117.3(127)	+74.5	---a	---	1033.7	+63.8	N-H bending in 1:2:NM::NH ₃ trimer
1144.2(119)	+101.4	---a	---	---a	---	
O=N=O Stretching						
1760.5(156)	---	1570.1	---	1572.7	---	v ₃ of NM monomer
1756.1(136)	-4.4	1565.3	-4.7	1568.4	-4.3	O=N=O stretch in NM-AM I dimer
1748.6 (174)	-11.9	---	---a	1568.4	-4.3	O=N=O stretch in NM-H ₂ O complex
1746.4(135)	-14.1	1555.9	-14.2	1564.8	-7.9	O=N=O stretch in 1:2:NM::NH ₃ trimer

Table 2: Comparison of shifts, in the signature absorptions by phosphorus trichloride and ammonia submolecules in heterodimers, predicted by harmonic frequency calculations and those observed in the IR spectra of matrix isolated samples

Computed Wavenumber (cm ⁻¹) ^a		Experimental Wavenumber (cm ⁻¹)				Mode Assignment
		Ar		N ₂		
v	Δv	v	Δv	v	Δv	
P-Cl Stretching						
483.1 (204)	-36.1	470.3/		463.1/		Asymm P-Cl stretch (ν_2) of PCl ₃ monomer
		467.9/	-31.0	461.4/	---	
509.5 (149)	-9.7	465.7		458.5	-35.6	N-H bending in 1:2:NM::NH ₃ trimer
		490.3	-8.7	---b		
N-H Bending						
1030.2 (143)	---	974.6	---	969.3	---	N-H bending (ν_2) of NH ₃ monomer
1075.6 (163)	+45.4	1004.0	+29.4	1017.3	+48.0	N-H bending in PAm I dimer

absorptions is dependent on the yield of heterodimers within the matrix. This is influenced by the relative proportion of the precursors and the IR absorption cross-section of the heterodimers, which in turn depends upon the strength of the interaction. Conscious manipulation of this proportion, on correlation with the observed intensities of absorption, forms unambiguous evidence of the generation of heterodimers within the matrix. The magnitude of

shift (in terms of wavenumbers, cm⁻¹) observed experimentally is compared with those predicted by harmonic frequency calculations on the specific geometries by *ab initio* and DFT methodologies (Tables 1 and 2). This agreement forms the evidence regarding the existence of heterodimers of interest.

Various possible geometries of heterodimers are optimized, by subjecting the respective wavefunctions (described by augmented–correlation consistent– polarized Valence Double/Triple Zeta basis sets) to Moller-Plesset second order perturbative treatments (MP2) and also using B3LYP and the state-of-the-art B2PLYP density functional methods. The optimized geometries represent critical points on the potential energy surface (PES) of heterodimers of which, that point corresponding to the global minimum would be the most favoured geometry energetically (Figure 4). The low temperature within the matrix ensures maximal generation of this favoured geometry. Heterodimers of nitromethane with NH₃ reveal the characteristic perpendicular orientation of the nucleophilic atom (nitrogen in NH₃) over nitrogen of nitromethane, relative to the O=N=O plane. In heterodimers of ammonia with phosphorus trichloride, the primary interaction driving the geometry was a Cl-P...N phosphorus bond. The specific anti-periplanarity adopted by the N-H bonds to the chlorine atoms of PCl₃ was also noted. These geometries correspond to the global minimum in the respective PESs. This preferential stabilization of the pnicogen bound structures in both the heterodimers has been elucidated further using various computational tools. Quantum theory of atoms in molecules (QTAIM) reveals the pairs (or triads and more) of atoms which are involved in interactions, by generating bond critical points (BCPs) at specific intermolecular coordinates (Figure 5). BCPs are features on the topology of electron density distribution in the space within heterodimers. The analysis reveals co-existence of pnicogen bonding with C-H...N hydrogen bonds in heterodimers of nitromethane with ammonia (NM-AM I) and also

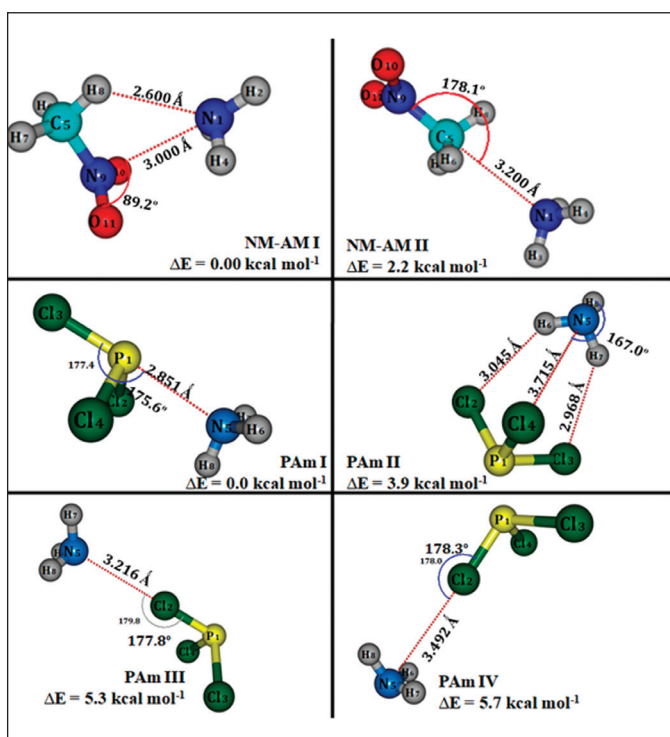


Figure 4. Geometries corresponding to the minima obtained on the potential energy surfaces, of heterodimers of ammonia with nitromethane (NM-AM) and with phosphorus trichloride (PAm), following optimization by MP2 treatment of respective wavefunctions described by aug-cc-pVQZ/pVTZ basis sets. The relative energies displayed have been extrapolated to complete basis set limits

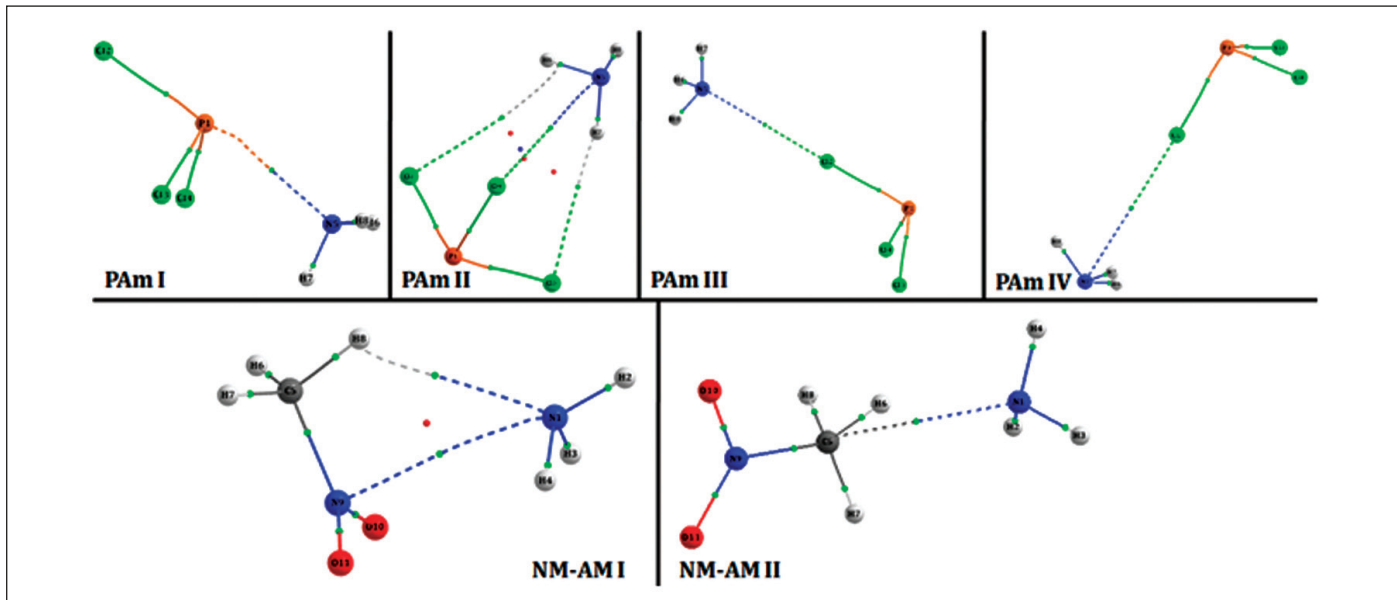


Figure 5. QTAIM plots of geometries corresponding to minima on the potential energy surfaces of PAm and NM-AM, displaying the pairs of atoms involved in intermolecular interactions. Green points represent BCPs while red ones correspond to ring critical points (RCPs)

the classic Cl-P...N phosphorus bond in heterodimers of ammonia with phosphorus trichloride (PAm I). The bond parameters at these BCPs namely, electron density (ρ), its Laplacian ($\nabla^2\rho$) and the total energy density (H), convey the greater strength of hydrogen bonds over pnicogen bonds in NM-AM. However, the respective geometries reveal a greater angular strain of hydrogen bonds, relative to the pnicogen bonds, which is the manifestation of characteristic directionality of the pnicogen bonds. QTAIM analysis reveals the interacting atoms but does not specify their electron accepting or donating character.

Natural Bond Orbital (NBO) analysis distinguishes the electron donor

and acceptor in an interacting pair by tracing the delocalization of electron density distribution between the atoms (Figure 6). A prominent delocalization of the non-bonded electron pair of nitrogen in NH_3 into the π^* anti-bonding molecular orbital (ABMO) of the $\text{O}=\text{N}=\text{O}$ moiety, via nitrogen is revealed, in the heterodimer of nitromethane with NH_3 . The co-existing hydrogen bond is also evident from the delocalization of the same non-bonded pair from NH_3 into the σ^* ABMO of the H-C bond of nitromethane. In PAm I dimer, the Cl-P...N phosphorus bond does manifest as the delocalisation of the non-bonded pair of nitrogen in NH_3 into the σ^* ABMO of the anti-periplanar P-Cl bond. Interestingly, a subtle back donation from the twin chlorine atoms (Cl_4 and Cl_2) into the σ^*

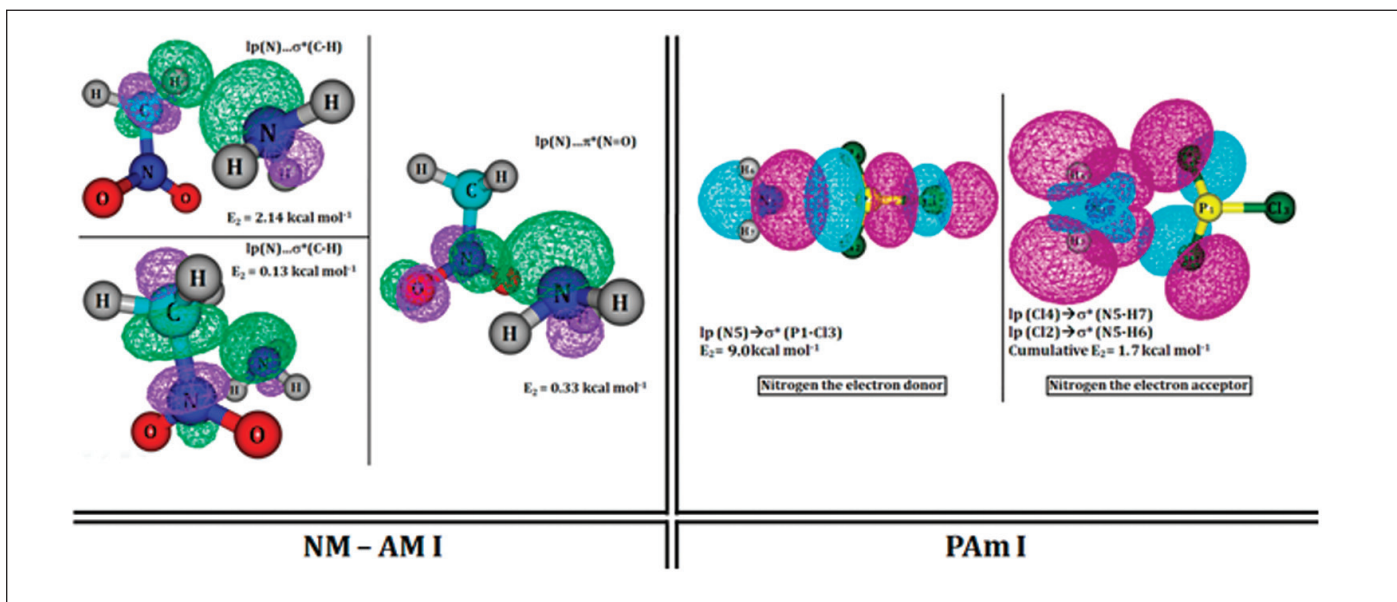


Figure 6. Spatial renditions of select natural bond orbitals displaying the delocalization of electron density in the intermolecular space within NM-AM and NM-PO

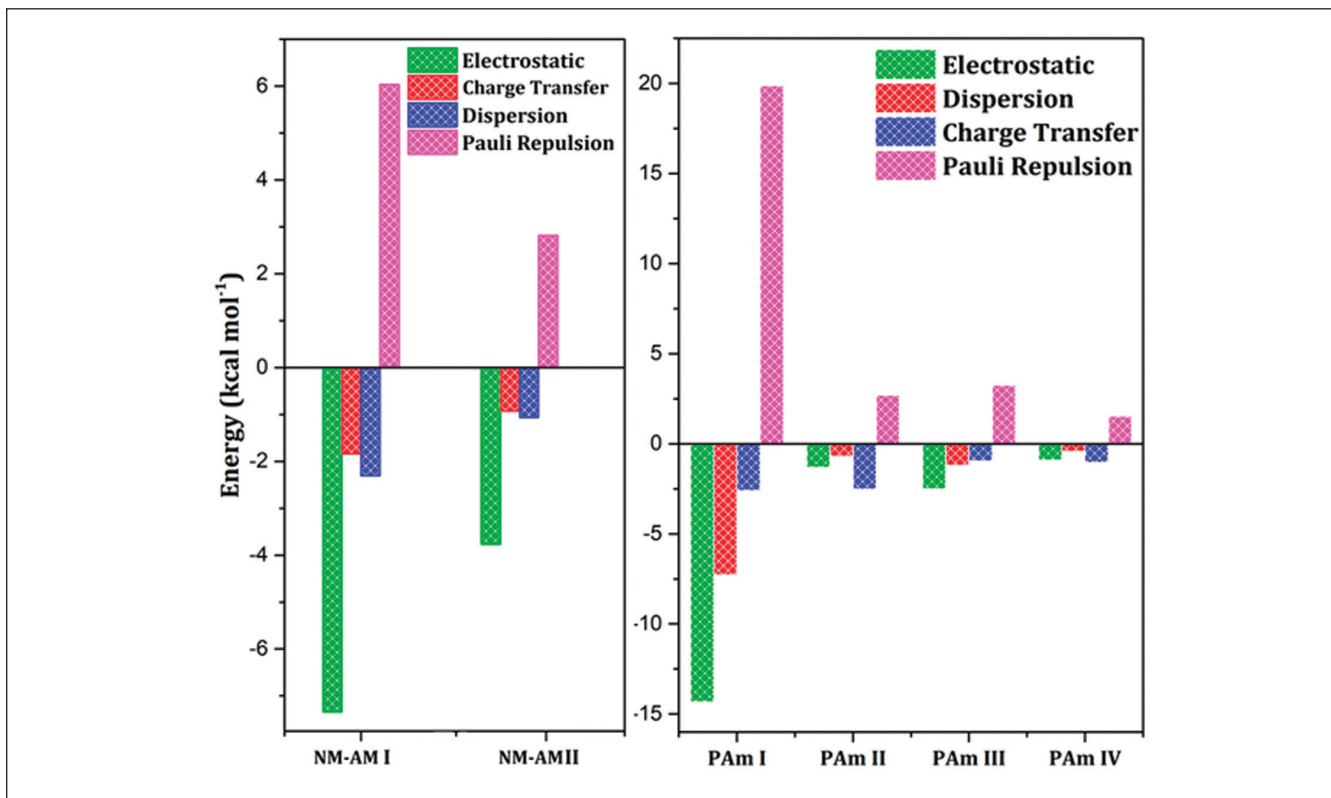


Figure 7. Graphical representation of results from energy decomposition analysis of the optimized geometries on potential energy surfaces of NM-AM and PAm

ABMOs of the N-H bonds located anti-periplanar, is also noted. This reveals the rather unexpected Lewis acidic role of nitrogen in NH₃. The binding energies associated with NM-AM and PAm dimers are decomposed into their contributions from various effects to comprehend the nature of interactions binding them.

The decomposition of binding energy associated with heterodimers into contributions from electrostatic, charge transfer and dispersion effects was performed by energy decomposition (ED) analysis using the Amsterdam Density Functional 2016 (ADF '16) package (Figure 7). The superior contribution of electrostatics, overwhelming those from dispersion and charge transfer was revealed for the heterodimers of nitromethane-NH₃. This instantly mitigated the anomalous angular strain of hydrogen bonds in favour of the pnicogen bonds in NM-AM. The rather uncharacteristic dispersive origins of the H-N...Cl pnicogen bonds is also observed in PAm I and II dimers.

The contribution of electrostatics, dispersion and charge transfer to hydrogen and pnicogen bonds have been fragmented in terms of the electron density, using non-covalent interaction (NCI) analysis. This reveals the hydrogen bonds to possess a much lower contribution from electrostatics relative to conventional hydrogen bonds. This in turn confirms the greater contribution from electrostatics seen in ED analysis to be reflective of the presence of the π -hole driven pnicogen bonds hosted by the electron accepting nitrogen of nitromethane. Interestingly in PAm dimers, the dispersion driven

origins of the H-N...Cl pnicogen bonds and the well-known electrostatic origins of the Cl-P...N phosphorus bonds are also reinforced by NCI analysis.

Alongside the experimental confirmation of the nature of O=N...N pnicogen bonds in NM-AM dimers, the H-N...Cl pnicogen bond was found to be dispersion driven unlike the pnicogen bonds discovered hitherto. This finding kindles questions about the supposed 'necessity' of anisotropies on the ESP and the primary role of electrostatics in sustaining pnicogen bonds. Such questions prove to be crucial and pivotal, given the impending 'definition' of the pnicogen bond by IUPAC.

In summary, pnicogen bonding alongside its counterparts, from the rest of p-block elements opens multiple avenues of research across disciplines. These weak interactions are instrumental in facilitating molecular recognition and stimulating biological activity, at the same time; occur quite frequently within inorganic macromolecules and crystal structures. The possible occurrence of pnicogen bonds even in the absence of electrostatic phenomena such as σ -/ π -holes like the H-N...Cl bond, widens the scope of their occurrence in real-time systems. Investigation of these phenomena also leads to questions regarding the completeness of our comprehension of certain fundamental chemical behaviours such as Lewis acidity and basicity and the very nature of a chemical bond.

National Hindi Scientific Seminar (NHSS-2022)

January 10, 2022



Director, IGCAR along with OLIC members releasing the abstract volume of NHSS-2022

On the occasion of World Hindi Day (10th January, 2022), the Official Language Implementation Committee (OLIC) of IGCAR & GSO jointly organized a two day National Hindi Scientific Seminar (NHSS-2022) on the theme of "SAMAJ-KALYAAN MEIN VIKIRAN EVAM NABHIKIYA PROUDYOGIKI KE ANUPRAYOG" (Applications of Radiation and Nuclear Technology for Societal Benefits) in hybrid mode on January 9-10, 2022. The seminar was conducted in Vikram Sarabhai Auditorium, IGCAR with more than 75 participants from IGCAR, GSO and other DAE Units at Kalpakkam attending it physically. About 35 outstation participants joined virtually through Webex online platform mainly comprising Scientific & Technical Officers, Doctors and Researchers from various DAE units and other prestigious institutions, from different parts of the country. The objective of the seminar was to facilitate exchange and dissemination of information regarding the benefits of radiation and nuclear technologies and also to encourage the use of official language Hindi in scientific and technical presentations.

The seminar was inaugurated by Shri S. A. Bhardwaj, Former Chairman, AERB, Mumbai in online mode. In his inaugural address Shri Bhardwaj impressed upon the participants to make conscious efforts to increase the use of Hindi language in writing reports and other forms of official work. He also delivered a plenary talk titled 'SAMAJ KALYAAN EVAM VIKIRAN' (Societal Benefits of Radiation Technologies) in the first technical session, that followed the inaugural function. Dr. B. Venkatraman, Director, IGCAR & Chairman, OLIC delivered presidential address. He highlighted the contributions of DAE and its constituent units in various fields of science and technology and said that we are also successfully eliminating tons of carbon emissions, annually, by producing electricity through nuclear energy which is a clean and green energy. Dr. B. K. Nashine, Group Director, ESG, & Alternate Chairman, OLIC, IGCAR also shared the dais as a guest of honour. In his address, Dr. Nashine expressed happiness over holding of the Hindi Seminar at a time when the country is celebrating Azadi Ka Amrit Mahaotsav to commemorate its 75th year of independence and said that we should take pride in propagating our scientific achievements among the masses through the medium of our own languages. Earlier, the inaugural function started with welcome address by Dr. Awadhesh Mani, SO/H & Convener, NHSS-2022 who also presented brief details of the seminar. The inaugural session concluded with vote of thanks by Dr. Vani Shankar, SO/G & Co-convener, NHSS-2022.

During this two-day seminar, a total of 29 technical presentations highlighting various applications of radiation in different fields like agriculture, energy, food preservation, health, industry, medicine, research & development and technology transfer were made in four technical sessions including 1 plenary lecture, 5 keynote addresses, 7 invited talks and 16 contributory presentations. The guests lecturers, contributory presenters and other participants hailed from different units like AIIMS, JAMIU (New Delhi); AERB, BARC, DAE, TMC (Mumbai); NPCIL (Rawatbhata), IPR (Gandhi Nagar), RMP (Mysore), ECIL (Hyderabad), RRCAT (Indore), IREL (Manavalakuruchi), MSME_DI (Chennai), IGCAR, GSO, BHAVINI, BARC-F, SRI/AERB (Kalpakkam). The technical sessions were chaired by Dr. B. K. Nashine, Director, ESG, Shri Tanmay Vasal, Head, PPCD/RDTG, Dr. N.V. Chandra Sekhar, Associate Director, MSG and Dr. Sekhar Kumar, Head, RPOD/RpG who also conducted the valedictory session in which the outcomes of the seminar was discussed and feedback obtained from the participants. NHSS-2022 successfully concluded with the vote of thanks by the Convener, followed by national anthem and group photography of physical participants, chairpersons and members of the organising committee.

*Reported by
Dr. B. K. Nashine, Group Director, ESG*

International Conference on Recent Advances in High Pressure Science and Technology (ICReAch-2022)

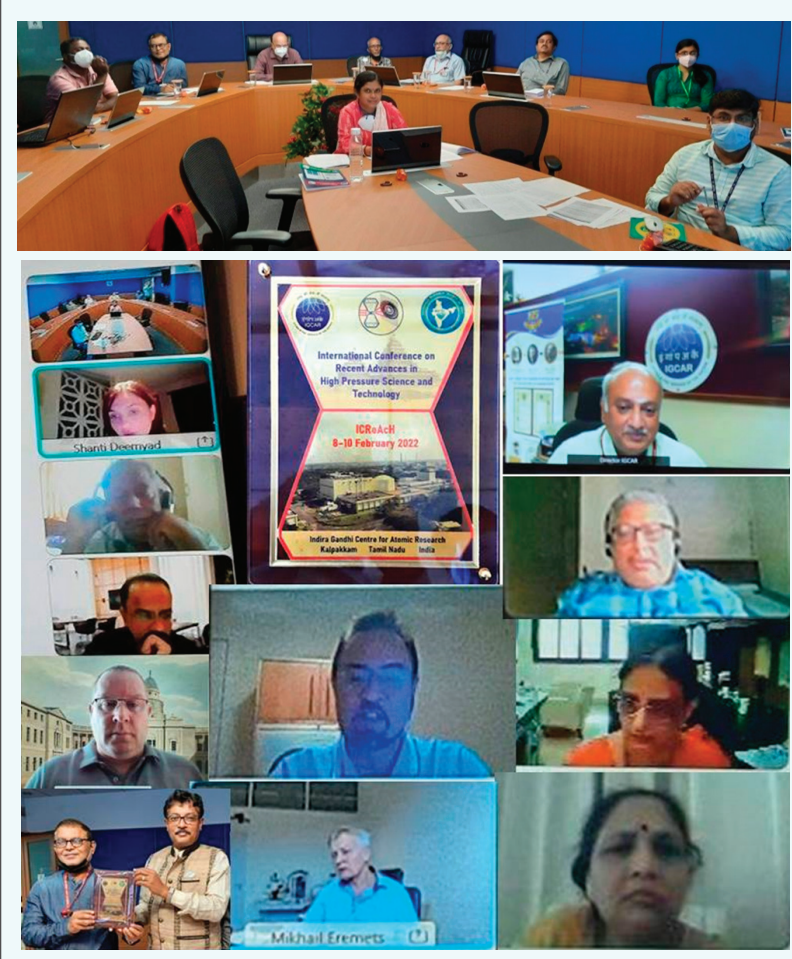
8-10 February 2022



Release of souvenir at the ICReAch-2022 conference

An International Conference on Recent Advances in High Pressure Science and Technology (ICReAch-2022) in online mode was held by IGCAR during 8-10 February 2022 from the Blue Room, Homi Bhabha Building. After the Welcome address by the Convener of the Conference Dr. N. V. Chandra Shekar, Associate Director, MSG, an overview of the Conference was given by the Chairman Dr. S. Raju, Director, Materials Science Group. The Conference was inaugurated by Dr. B. Venkatraman, Director, IGCAR, who released the Conference Abstracts book and delivered his Inaugural address. Dr. Venkatraman recalled the pioneering and seminal contributions of Nobel Laureate Percy William Bridgman to this field of research, and discussed the importance and relevance of high pressure research to DAE. In this Conference there were 3 Plenary Lectures, 23 Invited Talks, 28 Oral and 22 Flash Presentations, out of which 15 were from abroad (9 Europe, 5 US, 1 Japan). There were talks on high pressure studies on multiferroics, phase transformations, first principles computations, crystallography, thermodynamics of alloying, high temperature superconductivity, plastic strain induced phase transformations using rotational diamond anvil cell, high pressure synthesis of super hard materials, among other things. The technical sessions started with a Plenary Lecture by Professor Gautam Dev Mukherjee from IISER, Kolkata on Pressure induced re-entrant multiferroic/ferroic behaviour in certain oxide systems such as Fe₄Nb₂O₉. This was followed by an invited talk by Prof. A. Sundaresan from JNCASR, Bengaluru, on HP Synthesis of doubly ordered perovskites NaYMnO₆ and NaYNiO₆, and their multiferroic properties. Dr. Ranjan Mittal gave a detailed presentation of phase transition mechanism of hexagonal graphite to hexagonal and cubic diamond using ab-initio calculations. Prof. Chris Pickard from the University of Cambridge, UK, described his new approach to map the complex chemistry of dense matter, and ab-initio random structure searching using data-driven, machine learning algorithms. Prof. Shanti Deemyad from the University of Utah talked on her research on quantum effects that affect the structural phase transitions of lithium at low temperature. Prof. Ganapathy Vaitheeswaran from the University of Hyderabad presented the results of his ab-initio calculations on pressure induce metallization of solid iodanil (C₆I₄O₂), that becomes a metal at ~22 GPa. Prof. Leonid Dubrovinsky from Bayreuth University spoke on their development of a portable laser heating system with which they have studied a number of oxides, silicates and carbonates that are of geophysical importance. Dr. Subramanian Raju, Director, Materials Science Group and Metallurgy and Materials Group, IGCAR, presented an analysis of thermodynamics of materials under pressure, and stressed on the importance of high pressure

calorimetric measurements that are scant in the literature. Dr. Mikhail Eremets from Max Plank Institute for Chemistry, Germany, reviewed the status of research on superconductivity near room temperature, including his group's work on metal hydrides and pure hydrogen. Prof. Malcolm McMahon from the University of Edinburgh, spoke of the high pressure "collapsed" phases of lanthanide elements that were reported to be monoclinic. However, the diffraction data from these phases are not well fitted by the monoclinic structure. The collapsed phases of Tb, Gd, Dy, Ho, Er and Tm have a 16-atom orthorhombic structure ($\text{oF}16$) not previously seen in the element. Dr. Alexander Goncharov talked on the synthesis and properties of novel polyhydride and polynitride materials at high pressure and high temperature; these materials are potentially ultrahard, energetic or superconducting. Prof. Valery Levitas gave a detailed presentation of his group's work on plastic strain induced phase transformations under high pressure using rotational diamond anvil cell, and how plastic



The webinar was attended by senior scientists and engineers

shear reduced graphite to diamond phase transition pressure drastically from 70 GPa to 0.7 GPa. In the concluding session, Dr. S. Raju and Dr. N. V. Chandra Shekar, and General Secretary Dr. Awadhesh Mani shared their thoughts on the Proceedings, and hoped that this Conference will not be a one-off event, and other active Groups will take up organizing this periodically. Dr. T. R. Ravindran summarized the talks given in the Conference, giving a snapshot of the Proceedings. After this, winners of five Best Oral Presentations and five Best Flash Presentations in the Conference were announced by Dr. Raju. Evaluation was based on the clarity of presentation and quality of research content as adjudged by a panel of eminent scientists; Certificates and mementos were sent to the Winners by regular mail. The Conference concluded with Vote of Thanks by Dr. N. R. Sanjay Kumar.

*Reported by
Dr. Awadhesh Mani, Material Science Group*

Theme Meeting on Computational Modelling of Nuclear Reactor Materials

March 10, 2022



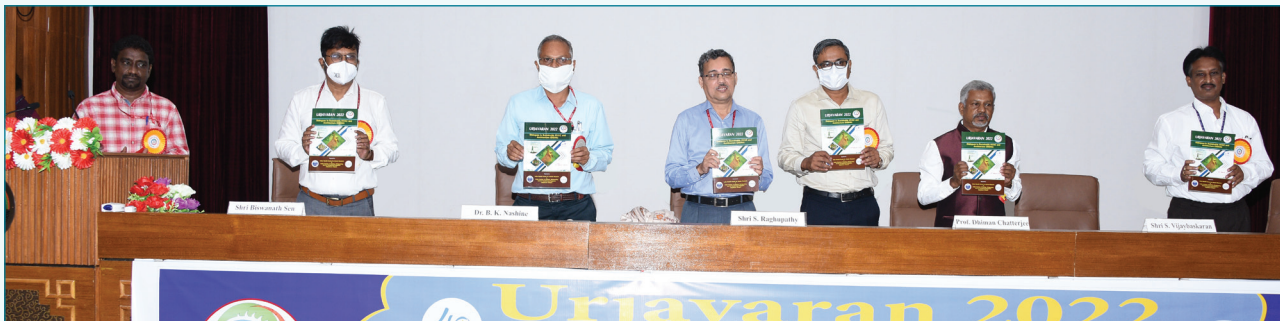
Few photographs of the online meeting on Computational Modelling of Nuclear Reactor Materials

A theme meeting on “Computational Modelling of Nuclear Reactor Materials” was held on 10th March, 2022 virtually at IGCAR. The meeting was inaugurated by Dr. N. V. Chandra Shekar, Associate Director, MSG, while Dr. R. Govindaraj, Head, DDSD, MSG briefed about the theme of the meeting. The objective of the theme meeting was twofold, firstly to explore areas of challenges in treating the nuclear materials computationally and the way forward and secondly to explore areas of possible collaboration in these areas. The theme meeting concentrated on techniques like the modelling of the properties the density functional theory (DFT), molecular dynamics (MD), Monte-Carlo and numerical simulations. The speakers, from BARC, IIT and IGCAR, made presentations on their work. Dr. Ashok Arya, BARC Mumbai talked on thermal behaviour of $(U,Np)O_2$ and $(Th,Np)O_2$ mixed oxides using DFT and MD. Dr. Manoj Warrier, BARC Vizag, talked about characterising extended defects like dislocations and dislocation loops that formed under ion irradiation using MD. Dr. Sharat Chandra gave an overview of the computational activities in MSG, IGCAR and Dr. J Christopher presented the numerical modelling of stress in steels while subjected to deformation and damage. Dr. C Ravi spoke about the thermodynamics of point defects in bcc Uranium, while Dr. Gurpreet Kaur talked about her work on phase stability of Uranium, Uranium compounds and intermetallics using DFT. Prof. Anoop Krishnan, IIT Delhi, covered the use of AI/ML in design of glasses of required composition and properties and generation of relational scientific database using the materials-aware language model, MatSciBERT. Dr. G. Gopakumar, talked about modelling the actinide separation and recovery processes in nuclear fuel cycle using quantum chemical methods. Mr. Shakti Singh talked about using Monte-Carlo methods to obtain accurate atomistic descriptions of silica and iron phosphate glasses, while Dr. Manan Dholakia presented his work on modelling the damage in many oxides which are used in ODS steels and for waste immobilization using MD. All the talks held in two sessions chaired by Dr. N. V. Chandra Shekar, AD, MSG and Dr. R. Divakar, AD, PMG respectively were followed by quite enlightening discussions from the present speakers and audience. Many important possibilities of collaboration emerged from these discussions. The meeting concluded with the vote of thanks by Dr. Sharat Chandra ,Head, MMS,DDSD. Thus the whole gamut of the nuclear fuel cycle, from structural materials like steels, nuclear fuel materials, separation and recovery of actinides during reprocessing and materials for waste immobilisation was covered during the meeting.

Reported by
Dr. R. Govindaraj and Dr. Sharat Chandra,
Materials Science Group

5th National Conference URJAVARAN – 2022

March 10, 2022



Release of souvenir during inaugural function: Shri T. V. Maran; Shri Biswanath Sen, Convener; Dr. B. K. Nashine, OS & Director - ESG; Shri S. Raghupathy, DS & Director - RDTG & EIG; Prof. Dr. Dhiman Chatterjee, IIT Madras; Shri S. Vijaybhaskaran, RD, ISHRAE HQ; and Shri V. Suresh Kumar, Organizing Secretary

Air-Conditioning & Ventilation System Division (AC&VSD), IGCAR organized the 5th National Conference URJAVARAN – 2022 in association with Indian Society of Heating Refrigerating & Air-conditioning Engineers (ISHRAE) - Kalpakkam Chapter at Sarabhai Auditorium on 10th March, 2022. The theme of the conference was “Dialogues In Sustainable HVAC and Architecture (DISHA)”. About two hundred and sixty delegates from various DAE units, academic institutions, industries and leading consultants attended the conference.

The conference started with the warm welcome address by convener Shri Biswanath Sen. The inaugural function was presided over by Shri S Raghupathy, Distinguished Scientist and Director, RTDG & EIG. In his presidential address, Shri. Raghupathy emphasized on reduction of CO₂ emission, implementation of climate policy and contribution of FBRs towards clean & green energy. He also stressed upon time limit for implementing the climate guidelines. Dr. B. K. Nashine, Outstanding Scientist & Director, ESG delivered the inaugural address and highlighted the significance of energy conservation for a sustainable environment. He has coined a new acronym “ACARA - Air-Conditioning As Reasonable as Achievable” and requested all to follow. Prof. Dr. Dhiman Chatterjee of IIT, Madras delivered the keynote address on “Vapor-liquid, two phase flow and phase change”. The address was interesting, intriguing and very relevant to the theme of the conference.

The Conference souvenir was released by Shri S. Vijaybhaskaran, Regional Director, South-II, ISHRAE HQ. Shri V. Suresh Kumar, Organizing Secretary proposed the vote of thanks. Shri A. Jyothish Kumar, OS & Director (Operations), BHAVINI and Dr. N. Sivaraman, OS & Director, MC&MFCG have inaugurated the exhibition stalls of exhibitors & industrial partners. Various industries, from the field of Heating Ventilation & Air Conditioning (HVAC) system and component design, showcased their products at the venue and shared specific features of their products.

The conference deliberated on the latest technologies, products and ongoing research on sustainable air conditioning and ventilation of buildings. Four invited talks were delivered by eminent speakers from academia, industries, R&D organizations, leading architects and consultants. Eighteen contributed papers from DAE units (IGCAR, BARCF, GSO), educational institutions and industries were presented covering wide spectrum like green building, automobile air-conditioning, concrete wall penetration cooling system, high temperature piping, including eleven posters. Shri J. K. Gayen, GM-Operations (BARCF), Dr. Kitheri Joseph, AD, MFRG, Shri. S. Vijaybaskaran, RD, ISHRAE HQ evaluated the posters. Product presentations from reputed industries were also a part of the conference. The conference facilitated good interaction among the delegates and experts in the area of sustainable HVAC.

During the valedictory function, Shri T. V. Prabhu, Convener, Technical Committee, summed up the one-day conference. Dr. K. Ananthasivan, OS & Director, RpG delivered the valedictory address. In his address he described the nuclear energy as green energy and emphasized on exploring energy conservation in air-conditioning & ventilation systems. Shri. M. Ravi, President Elect., ISHRAE Kalpakkam proposed the vote of thanks.

Reported by

*Shri Biswanath Sen, Convener, URJAVARAN – 2022
Engineering Services Group*

Awards, Honours and Recognitions

Dr.John Philip has been appointed as Associate Editor of International Journal of Ceramic Engineering and Science, American Ceramic Society, Wiley Publishers

Ms. Geethi Jena, CSTD, MMG has been awarded "NACE Foundation India Scholarship" of Rs.1,50,000/- by the NACE Foundation (USA)

Mr. Paulson Varghese, CSTD, MMG has been awarded "NACE Foundation India Scholarship" of Rs.1,50,000/- by the NACE Foundation (USA)

HBNI-IGCAR CI

Ph.D Thesis Defense

Name	Title	Discipline
Shri. Zaibudeen A. W.	Investigation on the Behavior of Stimuli-Responsive Macromolecules at Nanoemulsion Interface	Physical Sciences
Ms. Raktima Basu	Mechanism of Phase Transition in Vanadium Oxides and Its Applications	Physical Sciences
Shri Gopinath Sahoo	Surface Modification and Polymer-free Transfer of Vertical Graphene Nanosheets for Electrochemical Capacitor Applications	Physical Sciences

Bio-diversity @ DAE Campus, Kalpakkam

Paddyfield Pipit



© SIRD, IGCAR

Paddyfield Pipit is a slender terrestrial bird with pure white outer tail feathers, long legs, pointed bill, and long hind toes. Its eyebrow frequently appears to extend around-ear converts. It forages by running rapidly on the ground, wagging its tail, and has a weaker flight than other pipits.

Editorial Committee Members: Ms. S. Rajeswari, Dr. V. S. Srinivasan, Dr. John Philip, Dr. T. R. Ravindran, Dr. C. V. S. Brahmananda Rao, Shri A. Suriyanarayanan, Shri M. S. Bhagat, Shri G. Venkat Kishore, Dr. Girija Suresh, Shri M. Rajendra Kumar, Shri S. Kishore, Shri Biswanath Sen, Dr. N. Desigan, Shri Gaddam Pentaiah and Shri K. Varathan